Structure-Photophysics Correlations in a Series of 4-(Dialkylamino)stilbenes: Intramolecular Charge Transfer in the Excited State As Related to the Twist around the Single Bonds

Jean-François Lêtard,[†] René Lapouyade,*[,†] and Wolfgang Rettig[‡]

Contribution from the Laboratoire de Photophysique et Photochimie Molêculaire, URA du CNRS No. 348, Universitê de Bordeaux I, 351, cours de la Libêration, F-33405 Talence, France, and I.N. Stranski-Institute, Technische Universität Berlin, Strasse des 17. Juni 112, D-1000 Berlin 12, FRG. *Received September 11, 1992*

Abstract: 4-(Dimethylamino)stilbene and eight regioselectively bridged 4-(dialkylamino)stilbene derivatives have been synthesized and their solvatochromism, fluorescence quantum yields, and lifetimes measured versus the solvent polarity and the temperature. When the single bond connecting the dialkylanilino group to the ethylene group (bond 2) is bridged, strong fluorescence quenching is observed; when this bond is flexible, the fluorescence quenching is strongly reduced, and lifetime maxima at intermediate temperature indicate the involvement of a further TICT emitting state. Fluorescence quenching is reduced in polar solvents and suppressed when the double bond is included in a five-membered carbocyclic ring. This shows that the main deactivating step is connected with twisting of the double bond and that the double-bond twisted state is less polar than the emitting one.

1. Introduction

The photophysics and spectroscopy of donor–acceptor molecules which are capable of photoinduced intramolecular charge transfer (ICT) are the subject of continuing theoretical and experimental interest. There are many examples where conformational folding brings the donor and acceptor end groups into parallel planes within throughspace interaction distance resulting in a classical exciplex-type behavior,[1,2] but when the bridge is only one single bond, conformational folding is precluded and an orthogonal geometry, which minimizes the electronic interaction between the radical cation and radical anion, is often reached in the excited state.[3,4] This last type of compound has been studied extensively since Lippert et al.[5] discovered the dual luminescence of 4-(dimethylamino)benzonitrile in 1959 and since Grabowski et al.[6] (1973) assigned the long-wavelength emission to a rotational isomer in which a transfer of charge has taken place while the dimethylamino group has rotated into a plane perpendicular to that of the benzonitrile moiety (TICT). Whereas the importance of the cis-trans photoisomerization of the double bond in simple polyenes as well as in more complex visual pigments has been underlined and studied extensively, the rotation around a single bond as a source of intramolecular charge transfer in these compounds has scarcely been noted.[7,8] The simplest unit of a reasonably fluorescent ethylenic compound which can energetically lead to a TICT state is a donor–acceptor substituted stilbene.

We have recently embarked upon a detailed study of this class of compounds which led us to propose a three-state kinetic scheme (Figure 1) which in addition to state E* (planar geometry) and P* (double bond twist) contains a third state A* (single bond twist, TICT state) which is the state responsible for the main part of the emission.[7,9]

With selectively bridged derivatives of *p*-(dimethylamino)-*p'*-cyanostilbene (DCS) we have been able to locate the single bond around which the donor (dimethylanilino) and the acceptor (*p*-cyanostyrene) groups decouple (state A*) and to show that E* and A* states are highly polar while state P* is weakly polar.[7,9] With picosecond time resolved emission in highly concentrated solutions we have also observed a bicimer formation (aggregate of two excited molecules) linked to a head-to-tail complex in the ground state and to a TICT formation process in the excited state.[9-11]

Since the intramolecular formation of the TICT state of DCS occurs with a rate constant too fast to be resolved within 25 ps, which is the limit of resolution of our apparatus, we decided to increase the energy of the TICT (A*) state relative to that of the delocalized excited state (E*) of planar geometry by considering the (dimethylamino)stilbene (DS) series where the efficiency of the electron accepting part has been reduced relative to the DCS series by the removal of the cyano substituent. Additionally, in the ground state, DS is less polar than DCS (μg = 2.41 D[12] versus μg = 6.95 D for DCS[13]) and consequently should not aggregate so efficiently and should considerably differ in the picosecond range at high concentrations. Also, if derivatives of DS are structurally prevented from forming a TICT state, one could expect a less polar emissive E* state, whereas the polarities of E* and TICT states were comparable in the DCS series.[9]

2. Experimental Section

Most of the compounds I–X (Figure 2) were synthesized by reacting the corresponding ketones (or aldehydes) with Ti° ($TiCl_4$ + Zn) according to the Mc Murry method[14] as already described.[15] All the compounds were purified by column chromatography on silica gel followed by crystallization from petroleum ether and sublimation. They yielded satisfactory elemental analysis and MS, IR, and NMR spectroscopic data.

Solvents used were of spectrometric grade either from SDS (Solvants, Documentation, Synthèses) or from Merck (Uvasol or glass-distilled

[†] Universite de Bordeaux 1.
[‡] I.N. Stranski-Institute, Technische Universität Berlin.

(1) Beens, H.; Weller, A. *Organic Molecular Photophysics*; Birks, J. B., Ed.; Wiley: London, 1975; Vol. 2, p 159.
(2) DaVidson, R. S. *Advances in Physical Organic Chemistry*; Wiley; New York, 1983; Vol. 9, p 1.
(3) Rettig, W. *Angew. Chem. Int. Ed. Engl.* **1986**, *25*, 971 and references therein.
(4) Grabowski, Z. R.; Rotkiewicz, A.; Siemiarczuk, A.; Cowley, D. J.; Baumann, W. *Nouv. J. Chim.* **1979**, *3*, 443.
(5) Lippert, E.; Lüder, W.; Boos, H. In *Adv. Mol. Spectrosc. Int. Meet. 4th* Proc. European **1959**, 443.
(6) Rotkiewicz, K.; Grellmann, K. H.; Grabowski, Z. R. *Chem. Phys. Lett.* **1973**, *19*, 315; Erratum *Chem. Phys. Lett* **1973**, *21*, 212.
(7) Rettig, W.; Majenz, W. *Chem. Phys. Lett.* **1989**, *154*, 335.
(8) Rettig, W.; Majenz, W.; Lapouyade, R.; Haucke, G. *J. Photochem. Photobiol. A, Chem.* **1992**, *62*, 415.
(9) Lapouyade, R.; Czeschka, K.; Majenz, W.; Rettig, W.; Gilabert, E.; Rulliere, C. *J. Phys. Chem.* **1992**, *96*, 9643.
(10) Gilabert, E.; Lapouyade, R.; Rulliere, C. *Chem. Phys. Lett.* **1988**, *145*, 262.
(11) Gilabert, E.; Lapouyade, R.; Rulliere, C. *Chem. Phys. Lett.* **1991**, *82*, 185.
(12) Everard, K. B.; Kumar, L.; Sutton L. E. *J. Chem. Soc.* **1951**, 2807.
(13) Kawski, A.; Gryczynski, J.; Jung, C. H.; Heckner, K. H. *Z. Naturforsch.* **1977**, *32a*, 420.
(14) Mc Murry, J. E. *Chem. Rev.* **1989**, *89*, 1513.
(15) Letard, J. F.; Lapouyade, R.; Rettig, W. *Mol. Cryst. Liquid Cryst.*, in press.

0002-7863/93/1515-2441$04.00/0

Table I. Absorption and Fluorescence Maxima (in nm), Difference $\Delta\nu_{st}$ between Absorption and Fluorescence Maxima (cm^{-1}), Fluorescence-Band Half-Width $\Delta\nu_{1/2}$ (cm^{-1}), and Fluorescence Quantum Yields of DS and Bridged Model Compounds in Solvents of Different Polarity (Δf) at Room Temperature (experimental errors of Φ_f is ±10%)[a]

compds	solvent	Δf	λ_{abs}	λ_{fluo}	$\Delta\nu_{st}$	$\Delta\nu_{1/2}$	Φ_f
DS (I)	*n*-hexane	0	347	379	2433	3425	0.030
	Et_2O	0.167	349	407	4083	3600	0.029
	BuCl	0.209	352	418	4486	3327	0.042
	EtOH	0.289	348	433	5641	3689	0.035
	CH_3CN	0.305	351	440	5763	3306	0.037
DS-B1 (II)	*n*-hexane	0	347	396	3566	2986	
	Et_2O	0.167	350	422	4875	3262	0.054
	BuCl	0.209	354	435	5260	3308	0.054
	EtOH	0.289	348	454	6709	3616	0.032
	CH_3CN	0.305	352	466	6950	3356	0.056
DS-B2 (III)	*n*-hexane	0	352	388	2636	3712	
	Et_2O	0.167	354	398	3123	3375	0.002
	BuCl	0.209	357	404	3259	3352	0.002
	EtOH	0.289	355	418	4245	3855	0.002
	CH_3CN	0.305	358	435	4944	3521	0.002
DS-B4 (IV)	*n*-hexane	0	344	374	2332	3218	
	Et_2O	0.167	344	396	3817	3360	0.041
	BuCl	0.209	348	408	4226	3570	0.044
	EtOH	0.289	346	420	5092	3800	0.030
	CH_3CN	0.305	348	432	5587	3415	0.040
DS-B11 (V)	*n*-hexane	0	362	394	2243	2933	
	Et_2O	0.167	365	424	3812	3154	0.084
	BuCl	0.209	368	438	4343	3234	0.085
	EtOH	0.289	365	454	5371	3313	0.100
	CH_3CN	0.305	370	468	5660	3248	0.110
DS-B114 (VI)	*n*-hexane	0	358	387	2093		
	Et_2O	0.167	360	420	3968	2899	0.063
	BuCl	0.209	357	423	4370	3309	0.114
	EtOH	0.289	360	443	5204	3533	0.110
	CH_2CN	0.305	363	454	5522	3371	0.113
DS-B14 (VII)	*n*-hexane	0	344	386	3163	2716	
	Et_2O	0.167	346	413	4689	4805	0.034
	BuCl	0.209	350	422	4875	3386	0.038
	EtOH	0.289	348	439	5957	3584	0.029
	CH_3CN	0.305	350	454	6545	3265	0.044
DS-B34 (VIII)	*n*-hexane	0	340	395	4095	3608	
	Et_2O	0.167	343	409	4705	3640	0.714
	BuCl	0.209	344	412	4827		0.770
	EtOH	0.289	342	422	5571	3584	0.670
	CH_3CN	0.305	345	439	6206	3308	0.879
DS-B24 (IX)	*n*-hexane	0	364	388	1700		
	Et_2O	0.167	364	401	2535	4251	0.001
	BuCl	0.209	367	405	2557	3944	0.002
	EtOH	0.289	364	409	3023	3994	0.002
	CH_3CN	0.305	365	431	4195	3786	0.002
DDS (X)	*n*-hexane	0	357	388	2238		
	Et_2O	0.167	360	399	2715	3994	0.447
	BuCl	0.209	364	406	2842	3513	0.554
	EtOH	0.289	364	416	3434	3712	0.399
	CH_3CN	0.305	366	422	3626	3587	0.565

[a] Excitation wavelength for all spectra, 350 nm. For solvent abbreviations see caption to Table II.

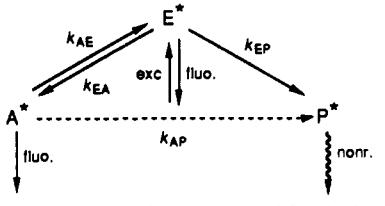

Figure 1. Three-state kinetic scheme proposed for the interpretation of the photophysical behavior of donor–acceptor substituted stilbenes.

quality). Butyronitrile (Fluka) was purified by column chromatography on alumina and subsequent distillation.

Absorption spectra were determined on a Varian CARY 219 spectrometer and fluorescence spectra on a Fluorolog Spex 212. The standard for the fluorescence quantum yield determinations with solvent refractive index correction was quinine bisulfate in 1 N H_2SO_4 (Φ_f = 0.55) and the experimental errors are ±10%. The excitation wavelength was 350 nm and the optical density was lower than 0.1. All the solutions were non-degassed.

Fluorescence decay times with a resolution down to about 100 ps and a high dynamic range (>10^4) were measured using a single-photon counting setup described in detail elsewhere.[16] The statistical error for every lifetime measurement is smaller than 0.1 ns. For excitation, synchrotron radiation from BESSY in the single bunch mode was used. We have checked that under our experimental conditions the lifetime and quantum yield values were not affected by repeated measurements of the same solution, such that cis-product formation can be neglected for our experiments.

3. Results

(1) Steady-State Spectra. (a) Electronic Absorption Spectra. The ultraviolet–visible spectra of DS and of the bridged model compounds are summarized in Table I. The absorption spectra of compounds II–X are similar to that of I (DS) and resemble that of stilbene (simulated by the protonated DS) with a considerable bathochromic shift (Figure 3) suggesting some degree of charge transfer interaction. However, the small bathochromic shift with increasing solvent polarity (Figure 3) is consistent with a weak difference between the dipole moments of Franck-Condon excited and ground states.

(16) Vogel, M.; Rettig, W. *Ber. Bunsenges. Phys. Chem.* **1987**, *91*, 1241.

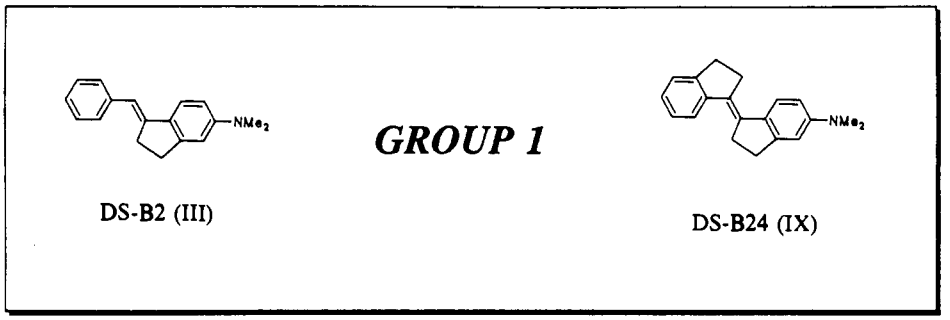

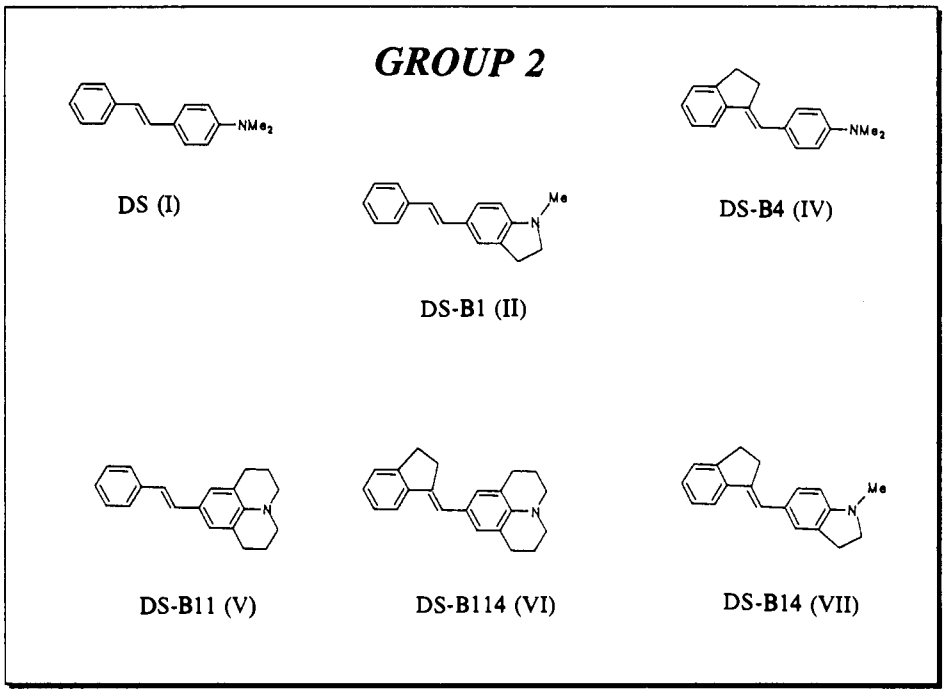

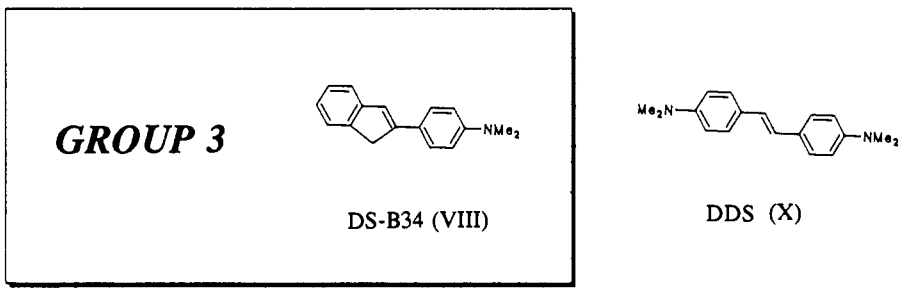

Figure 2. Molecular structure of DS and the bridged model compounds.

The positions of the absorption maxima λ_{abs} are collected in Table I. Compounds DS-B2 and DS-B24 show a bathochromic shift of about 5 and 15 nm in CH_3CN, respectively, as compared to DS which is probably the consequence of increased planarization of the system. On the other hand, the slight blue shift (5 nm) for DS-B34 indicates some steric interaction between the indene and the dimethylanilino groups. The red shift of about 15 nm observed for the julolidine compounds DS-B11 and DS-B114 is possibly also related to a planarization of the system, but this red shift is absent for the indoline-bridged system DS-B1. A similar behavior is exhibited for the correspondingly bridged derivatives of DMABN[17,18] and also for rhodamine and coumarine laser dyes.[19,20]

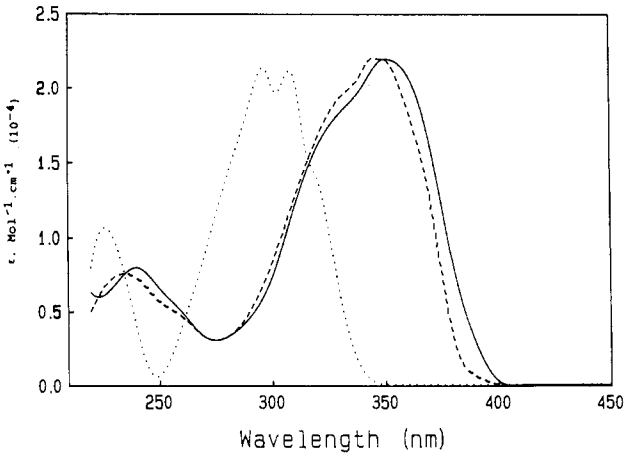

Figure 3. Absorption spectra of DS in *n*-hexane (---), acetonitrile (—), and ethanol + HCl (···) at T = 300 K and $c = 3 \times 10^{-5}$ M.

(17) Rettig, W.; Gleiter, R. *J. Phys. Chem.* **1985**, *89*, 4676.
(18) Rettig, W.; Rotkiewicz, K.; Rubaszewska, W. *Spectrochim. Acta* **1984**, *40a*, 241.
(19) Drexhage, K. H. Dye Lasers. In *Top Appl. Phys.* **1973**, *1*, 144.
(20) Brackmann, U. *Lambdachrome, Laser Dyes*; Lambda Physik GmbH: Göttingen, 1986.

Table II. Solvatochromic Slopes $m(1)$ (10^3 cm$^{-1}/\Delta f$), $m(2)$ (10^3 cm$^{-1}/\Delta f'$), $m(4)$ (10^3 cm$^{-1}/\Delta L'$) and Dipole Moments (D Units) of the DS Derivatives Obtained According to Equations 1, 2, and 4 Taking into Account the Five Solvents *n*-Hexane, Diethyl Ether, *n*-Butyl Chloride, Dichloromethane, and Acetonitrile Except for DS, DS-B2, DS-B34, and DS-B24, where Dibutyl Ether and Dimethylformamide Were Used Additionally

groups	compds	ρ^c (Å)	$m(1)$	μ_e	$m(2)$	μ_e'	$m(4)$	$\mu_e°$
1	DS-B2	4.70	2937[a]	7.8[a]	4453[a]	8.0[a]	4088	6.4
			16364[b]	15.2[b]	18107[b]	14.7[b]		
	DS-B24	4.86	4625[a]	9.6[a]	5322[a]	9.0[a]	3560	6.3
			16401[b]	15.9[b]	16699[b]	14.8[b]		
2	DS	4.53	11254	12.4	12335	11.8	5255	6.9
	DS-B1	4.61	11084	12.6	11996	11.9	5320	7.1
	DS-B4	4.70	10235	12.5	11184	11.8	5060	7.1
	DS-B11	4.86	11158	13.5	12597	13.1	5645	7.9
	DS-B114	5.01	11571	14.2	12450	13.5	5384	8.1
	DS-B14	4.78	10447	12.9	11913	12.5	5388	7.5
3	DS-B34	4.61	2486[a]	7.3[a]	5088[a]	8.2[a]	3212	5.5
			15784[b]	14.6[b]	14526[b]	13.0[b]		
4	DDS	4.81	4403	9.3	6540	9.7	2912	5.6

[a] Linear regression between *n*-hexane and *n*-butyl chloride. [b] Linear regression between *n*-butyl chloride and acetonitrile. [c] ρ is the equivalent cavity radius calculated from the molar volumes.

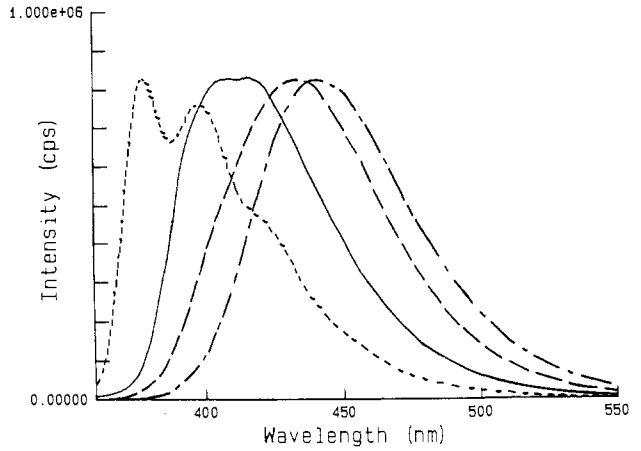

Figure 4. Normalized fluorescence spectra of DS in *n*-hexane (---), diethyl ether (—), ethanol (--), and acetonitrile (-·-) at room temperature.

(b) Fluorescence Studies. Figure 4 shows normalized fluorescence spectra of DS, measured in solvents of different polarity. In polar solvents, the spectra are completely structureless and strongly red shifted. The position of the fluorescence emission maximum (λ_{fluo}), the Stokes shift ($\Delta\nu_{st}$), the fluorescence-band half-width ($\Delta\nu_{1/2}$), and the fluorescence quantum yield (Φ_f) are presented in Table I.

The difference between the ground and the excited state dipole moments $\Delta\mu_{eg}$ can be calculated using the Lippert[21] eq 1

$$\Delta\nu_{st} = \nu_{abs} - \nu_{fluo} = 2\Delta\mu_{eg}^2\Delta f/hc\rho^3 + \text{Const} \qquad (1)$$

where $\Delta f = [(\epsilon - 1)/(2\epsilon + 1)] - [(n^2 - 1)/(2n^2 + 1)]$ represents a measure for solvent polarity and polarizability, defined respectively by the dielectric constant ϵ and the optical refractive index n. The slope m of a plot of $\Delta\nu_{st}$ versus Δf gives the value of $2\Delta\mu_{eg}^2/hc\rho^3$. The magnitude of $\Delta\mu_{eg}$ may be obtained from the slope by estimating the value of the cavity radius ρ (values between 4.53 and 5.01, see Table II) from the molecular volume as calculated from the molecular weight and the density of 0.95 g·cm^{-3} of *N*,*N*-dimethylaniline. Adding the experimental ground state dipole moment of DS (2.41 D)[12] yields μ_e for compounds I–X (Table II). Equation 1 assumes the Franck-Condon excited state reached upon absorption and the relaxed emitting excited state to be of the same nature. This assumption is not always fulfilled in our case, at least where the possibility for TICT formation exists and where the excited state reached upon absorption (E*) is considerably less polar than the emissive TICT excited state (A*). With the assumption of equal polarizabilities in the ground and the excited states we therefore also determined the excited-state dipole moment μ_e' accessible after Mataga[22] and Liptay[23] from the fluorescence solvatochromic shift alone according to eq 2

$$\nu_{fluo} = -2\mu_e'(\mu_e' - \mu_g)\Delta f'/hc\rho^3 + \text{Const}' \qquad (2)$$

with $\Delta f' = (\epsilon - 1)/(2\epsilon + 1) - 0.5(n^2 - 1)/(2n^2 + 1)$. The excited-state dipole moments obtained from eqs 1 and 2 are collected in Table II. All the compounds have a Stokes shift ($\Delta\nu_{st}$) which increases linearly with Δf (correlation coefficient $R > 0.98$), except DS-B2, DS-B24, and DS-B34, where two regions with different slopes are apparent (Figure 5a).

Equations 1 and 2 take into account the reaction field caused by the polarization of the surrounding solvent (which is considered as an isotropic continuum) by the solvent-dependent dipole of the solute itself. The solvent-polarity dependence of μ_e or μ_e' is brought about by the solute polarizability α_e according to eq 3[23,24]

$$\mu_e' = \mu_e°/(1 - f\alpha_e) \qquad f = 2(\epsilon - 1)/(\rho^3(2\epsilon + 1)) \quad (3)$$

where $\mu_e°$ is the permanent electric dipole moment of the solvent free molecule in the fluorescent state. The experimental value of μ_e' in polar solvents may be considerably larger than $\mu_e°$. For the assumption of an intermediate polarizability $\alpha_g \approx \alpha_e \approx 0.5\rho^3$ between that of the ground state of aromatics ($\alpha_g \approx 0.3\rho^3$) and that of the more polarizable TICT states, and by neglecting the dipole moment of the ground state ($\mu_g = 0$ D) the excited-state dipole moment $\mu_e°$ can be directly determined by the plot of ν_{fluo} versus $\Delta L'$ according to eq 4[25-27]

$$\nu_{fluo} = -2\mu_e°^2\Delta L'/hc\rho^3 + \text{Const}'' \qquad (4)$$

with

$$\Delta L' = (\epsilon - 1)/(\epsilon + 2) - 0.5(n^2 - 1)/(n^2 + 2)$$

The excited-state dipole moments estimated according to eq 4 are collected in Table II. The values of μ_e and μ_e' obtained from eqs 1 and 2 are almost the same. The excited-state dipole moment of DS ($\mu_e' = 11.8$ D) is slightly lower than that of all the other compounds (11.8 D $< \mu_e' <$ 13.5 D) with a linear dependence of Δf or $\Delta f'$ (DS-B1, DS-B4, DS-B11, DS-B14, DS-B114). The μ_e' values, which include the induced dipole moment, are significantly larger than those corresponding to the dipole moments of the free molecule $\mu_e°$ (11.8 versus 6.9 D for DS).

(21) Lippert, E. *Z. Naturforsch.* **1955**, *10a*, 541.
(22) Mataga, N.; Kaifu, Y.; Koizumi, M. *Bull. Chem. Soc. Jpn.* **1956**, *29*, 465.
(23) Liptay, W. *Z. Naturforsch.* **1965**, *20a*, 1441.
(24) Baumann, W.; Bischof, H.; Fröhling, J. C.; Brittinger, C.; Rettig, W.; Rotkiewicz, K. *J. Photochem. Photobiol. A, Chem.* **1992**, *64*, 49.
(25) Bilot, L. U.; Kawski, A. *Z. Naturforsch.* **1962**, *17a*, 621.
(26) Rettig, W. *J. Mol. Struct.* **1982**, *84*, 303.
(27) Herbich, J.; Kapturkiewicz, A. *Chem. Phys.* **1991**, *158*, 143–153.
(28) Leinhos, U.; Kühnle, W.; Zachariasse, K. A. *J. Phys. Chem.* **1991**, *95*, 2013–2021 and references therein.

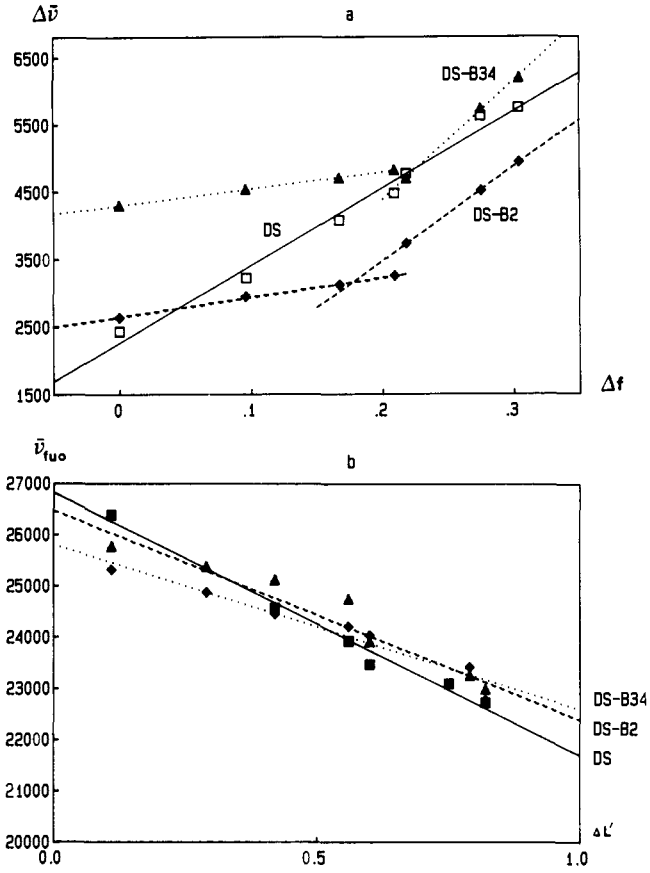

Figure 5. Solvatochromic plot of Stokes shift for several compounds. The solvent polarity function $f(\epsilon,n)$ corresponds to eq 1 (a) and eq 4 (b): (—) DS, (---) DS-B2, (···) DS-B34.

For DS-B34, DS-B24, and DS-B2 the solvatochromic plots of ν_{fluo} versus Δf and $\Delta f'$ give two slopes (according to eq 1 or 2), but only one (Figure 5b) if plotted according to eq 4. This may indicate that in this case the curvature of the solvatochromic plot according to eqs 1 and 2 observed with nonpolar solvents is only due to polarizability effects.

(c) Quantum Yields. The quantum yield of fluorescence Φ_f of DS and of the bridged model compounds in different solvents are shown in Table I. A small increase of Φ_f with the polarity of the solvent can be noticed in the majority of cases, with ethanol mostly leading to smaller Φ_f values than expected from the comparison to aprotic polar solvents.

Contrary to the small differences found for the various model compounds in the spectral properties for absorption and emission, the quantum yields differ strongly (table I). DS-B2 and DS-B24 (group 1), where the single bond connecting the dimethylanilino group to the central double bond is bridged, show by far the lowest quantum yield ($\Phi_f \leq 0.002$). DS, DS-B1, DS-B4, DS-B11, DS-B14, and DS-B114 (group 2 where the single bond in position 2 is free to rotate) show intermediate quantum yields characteristically lower in Et_2O (DS $\Phi_f = 0.03$) than in CH_3CN ($\Phi_f = 0.052$ for DS), and DS-B34 (group 3), with the double bond rigidly bridged, shows quantum yields of about 0.8 in all solvents investigated. Interestingly, a nearly comparable increase of the quantum yield as for DS-B34 can be obtained by introducing a second donor substituent ($\Phi_f = 0.57$ for DDS in CH_3CN), while adding an acceptor substituent as in DCS changes Φ_f only moderately ($\Phi_f = 0.11$ for DCS in CH_3CN[9]).

(2) Time-Resolved Measurements. The room and low-temperature fluorescence lifetimes in different solvents are shown in Table III.

Similarly as defined in connection with the quantum yield three categories can be discerned at room temperature (300 K). The members of group 1 (DS-B2, DS-B24) in both highly and weakly polar solvents each have a fluorescence lifetime too short for the detection limit of our single photon counting setup (<100 ps). In all the solvents investigated the compounds of group 2 have a lifetime around 0.1–0.2 ns and for DS-B34 (group 3) a long fluorescence lifetime is observed (1.9 ns in ethanol).

Lowering the temperature normally reduces any temperature-dependent nonradiative process k_{nr} which competes with fluorescence from an emitting state, say E*. An increasing fluorescence lifetime (or quantum yield) results up to a constant maximal value when the solvent becomes glassy. The flexible model compounds generally conform to this picture with several subtleties, however (Figure 6 and 7).

In group 1, the fluorescence decays of DS-B2 are decreasing from 1.9 ns at 77 K to 0.2 ns at 163 K. At 148 and 123 K, i.e.

Table III. Fluorescence Decay Times (ns) of DS and Bridged Model Compounds in Ethanol and Diethyl Ether at Room Temperature (Uncertainty in τ_f is ±0.1 ns)

Ethanol

group	compds	300 K	263 K	223 K	193 K	163 K	148 K	123 K	77 K
1	DS-B2[a]	<0.1	<0.1	<0.1	<0.1	0.2	0.6	1.5	1.9
	DS-B24	<0.1	<0.1	<0.1	<0.1	0.1	0.4	1.5	1.7
2	DS	0.1	0.2	0.8	1.5	1.9	1.9	1.8	1.7
	DS-B1	0.1	0.7	1.1	1.6	1.7	1.7	1.6	1.9
	DS-B4	<0.1	0.2	0.7	1.5	1.8	1.7	1.6	2.2
	DS-B11	0.3	0.7	1.5	2.0	1.8	1.9	2.0	2.0
3	DS-B34	1.9	2.0	2.0	1.9	2.0	1.9	1.7	1.9
4	DDS	1.0	1.6	1.7	1.8	1.7	1.7	1.7	1.8

Diethyl Ether

group	compds	300 K	253 K	223 K	193 K	163 K	77 K
1	DS-B2[a] (III)	<0.1	<0.1	<0.1	<0.1	0.1	1.9
	DS-B24 (IX)	<0.1	<0.1	<0.1	<0.1	0.3	1.8
2	DS (I)	0.1	0.4	0.7	1.4	1.7	1.7
3	DS-B34 (VIII)	1.8	1.6	1.7	1.7	1.9	1.9

[a] DS-B2 can be considered monoexponential with a slight impurity.

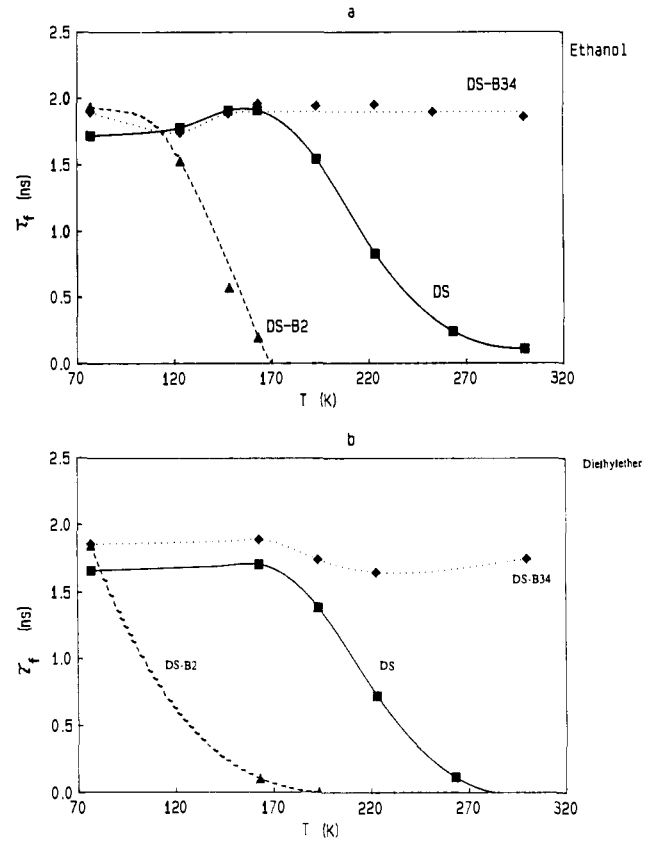

Figure 6. Plot of the fluorescence lifetimes (ns) versus temperature (K) in ethanol (a) and in diethyl ether (b) for DS (—), DS-B2 (---), and (···) DS-B34.

Table IV. Fluorescence Decay Times (ns) of DS, DS-B2, DS-B4, and DS-B34 in Ethanol and Diethyl Ether at 223 K and at Reference Temperature T_{ref} and Derived Radiationless Decay Rate Constants k_{nr} (10^7 s^{-1}) at 223 K (and 163 K for Group 1)

group	compds	solvent	T_{ref} (K)	τ_{fref}	τ_{f223K} (k_{nr})	τ_{f163K} (k_{nr})
1	DS-B2	Et_2O	77	1.9	<0.1 (>9500)	0.1 (9470)
		EtOH		1.9	<0.1	0.2 (4740)
	DS	Et_2O	77	1.7	0.7 (84)	
		EtOH	156[a]	1.9	0.8 (72)	
2	DS-B1	EtOH	163	1.7	1.1 (32)	
	DS-B4	EtOH	163	1.8	0.7 (87)	
	DS-B11	EtOH	193	2.0	1.5 (17)	
3	DS-B34	EtOH	163	2.0	2.0 (0)	

[a] Intermediate between 148 and 163 K.

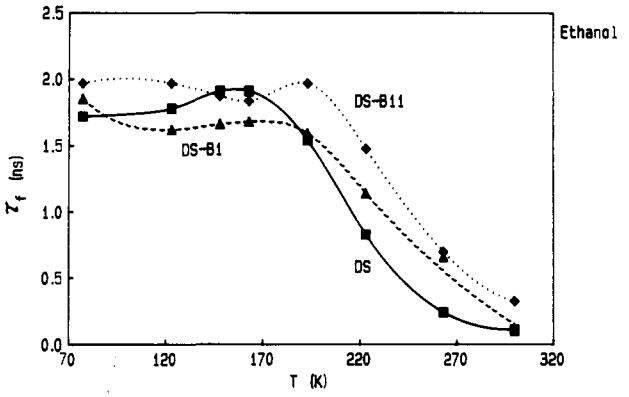

Figure 7. Plot of the fluorescence lifetimes (ns) versus temperature (K) in ethanol for DS (—), DS-B1 (---), and DS-B11 (···).

below the glass transition temperature of ethanol, the lifetimes are intermediate (0.6 and 1.5 ns, see Figure 6a). In diethyl ether (Figure 6b) the same behavior is observed but with an even shorter lifetime at 163 K (0.1 ns). DS-B24 behaves similarly with lifetimes <0.5 ns at 163 K (see Table III).

The compounds of group 2 behave abnormally in ethanol (example of DS in Figure 6a). From low temperatures of the alcoholic solution (77–163 K) to intermediate temperatures (156–190 K), they show a lifetime increase (for DS τ_f = 0.2 ns). Such a behavior with a lifetime maximum at intermediate temperatures has been previously observed for DCS[9] (increase of 0.5 ns from 77 to 160 K). At higher temperatures (until room temperature), the lifetimes shorten as usual but values below 0.5 ns occur only at $T > 223$ K for DS. The fluorescence lifetime maxima occur at different temperatures for DS (156 K), DS-B1 (171 K), and DS-B11 (190 K) (Figure 7). Also from 77 K an initial decreasing lifetime is observed when the temperature increases to 123 K (DS-B1, DS-B4) and even 163 K (DS-B11). In low polarity solvents (diethyl ether) the compounds of group 2 (DS, Figure 6b) present no lifetime maxima but a decrease of the fluorescence lifetimes versus the temperature from 163 K (1.7 ns) to 300 K (<0.1 ns).

DS-B34 (group 3) in polar solvent (ethanol, Figure 6a) shows a slight increase of lifetimes from 123 K (1.7 ns) to 163 K (2.0 ns) from where it remains virtually constant until room temperature (300 K, 1.9 ns). In a weakly polar solvent (diethyl ether, Figure 6b) DS-B34 also shows only slight variations of the lifetimes over the whole temperature range.

This contrasting behavior can be interpreted by using the three-state kinetic scheme. While group 1 compounds behave normally with only one emitting state E*, from the lifetime shortening of which we can calculate the reaction rate k_{nr} (see below), the initial low-temperature increase in lifetimes of the group 2 compounds, as the temperature is raised, can be interpreted by the formation of a new emitting species A* with longer intrinsic decay time than E*.[7-9] The increase of the lifetime is much stronger in the DCS derivatives[9] (0.5 versus 0.2 for DS) but the qualitative behavior is similar. At very low temperatures, A* formation is prevented by the rigid matrix which softens to allow molecular relaxation in the temperature range 120–170 K for ethanol, well visible by the strong lifetime decrease for DS-B2 (Figure 6a). In the same temperature range the lifetimes of DS increases. Above this temperature, the thermodynamic equilibrium between E* and A* can be attained, and the quenching reaction toward P* sets in also for DS and this leads to the lifetime maximum. For DS-B34 the initial behavior is qualitatively similar, and the slight decrease of lifetimes above 170 K (Table III) is consistent with the absence of the quenching reaction toward P* and a shift of the E* $\rightleftarrows$ A* equilibrium toward E* with increasing temperature. This indicates the energetically A* should be situated slightly below E*.

From the temperature dependence of τ, the non-radiative decay rate constant k_{nr} can be derived by using 5,

$$k_{nr}(T) = \tau_f^{-1}(T) - \tau_{f,ref}^{-1} \quad (5)$$

For a comparison of all three groups of compounds, we chose $\tau_f(T)$ at 223 K (where a large decrease of τ due to k_{nr} is already reached). As reference lifetime $\tau_{f,ref}$ we selected the lifetime maximum $\tau_{f,max}$ observed at different temperatures according to the compounds involved (for group 1 with the emitting state E* it is at 77 K but for group 2 and 3 compounds, the lifetime maximum is reached between 156 and 190 K in ethanol). The results are summarized in Table IV. We can notice an increase of k_{nr} when the polarity of the solvent decreases and a strong variation between the different groups of compounds ($k_{nr,group1} >>> k_{nr,group2} >>> k_{nr,group3}$). Within group 2, successive bridging of the dimethylamino group (DS, DS-B1, DS-B11) slows down k_{nr}.

4. Discussion

The results of the solvatochromism, of the fluorescence quantum yields, and of the lifetimes versus the solvent polarity and the temperature can be discussed within the three-state model presented above.

All the compounds of the (dialkylamino)stilbene series can be divided into three groups. Group 1 corresponds to the compounds where the single bond connecting the dimethylanilino group to the double bond is bridged (DS-B2, DS-B24): in ethanol one emitting state (the initially reached E* state) is prevailing with a very low Φ_f and τ_f already at 163 K due to fast photoreaction (double bond twisting, deactivating step k_{EP} in the scheme, Figure 1). Nevertheless the two slopes observed in the solvatochromic plot according to eqs 1 and 2 (see Table II and Figure 5a) could indicate a solvent dependence of the nature of the emitting excited state. It is possible that the polar solvents sufficiently lower yet another TICT state, which is reachable by twisting bond one, where the dimethylamino group acts as the donor group (Table III). It could also be due to a planar charge transfer state as has been shown recently with the planar model compounds of DMABN.[28] In principle, these two mechanisms could be differentiated by comparing DS-B2 to the doubly bridged model compound DS-B12 (not yet available).

Group 2 gathers all the derivatives with a free single bond connecting the dimethylanilino group to the ethylenic double bond: an increase of the lifetime from the lowest temperature of the alcoholic solution to an intermediate temperature, is in favor of a kinetic conversion (k_{EA}) of the nature of the emitting state from E* to A*. The decrease of the lifetime at higher temperature corresponds to the deactivating step k_{AP} or ($k_{AE} + k_{EP}$). The increase of the temperature of τ_{max} from DS to DS-B1 and DS-B11

is due to a decrease of the rate constant k_{nr} in that order (Table IV) and is probably connected to the energetic lowering of the initial state E* of the bridged compounds (compare the red-shifted absorption, Table I) which will decrease k_{EP}. This relative energy lowering of the E* state can also explain the "normal" decreasing lifetime above 77 K before the A* state is reached, as observed for the group 1 derivatives.

The state P* is not available for DS-B34 (group 3) and the lifetime and the quantum yield of fluorescence are only weakly affected by the temperature and the solvent polarity. As a matter of fact the slight increase of the lifetime at around 160 K in ethanol and at 230 K in ether is in favor of an equilibrium between two emitting states (E* and A*).

The intramolecular fluorescence quenching rate constant, k_{nr}, measured at 223 K shows very clearly that the main deactivating step is the formation of P* connected with the rotation of the double bond ($k_{nr} \approx 0$ for DS-B34 and $k_{nr} \geq 9500.10^7\ s^{-1}$ for DS-B2 in EtOH). If the bridging bond in DS-B2 is taken away leading to increased molecular flexibility, the TICT state can be populated and k_{nr} is reduced by nearly two orders of magnitude ($k_{nr} = 72 \times 10^7\ s^{-1}$ in EtOH for DS). This provides a further example of a stabilization (lifetime lengthening) of the emitting excited state due to an increase of the dimensionality of the reaction hypersurface, which would be unexplainable by a two-state model.[8] On the other hand, if the dimensionality is affected by bridging a bond not connected to TICT formation (e.g. bond 4), the k_{nr} values are unaffected (compare DS and DS-B4 in Table IV, both of group 2). The k_{nr} rate constant decreases moderately with an increase of the solvent polarity, showing that E* and A* are more polar than the quenching state P*.

Compound X (DDS) with an additional dimethylamino group with respect to DS excells by its tenfold increased quantum yield although the absorption and fluorescence properties are rather similar (Table I). From the temperature dependence of the lifetimes (Table III) it may be calculated that there remains a residual quenching pathway k_{nr}. If it is attributed to quenching by P*, then the small k_{nr} values with respect to DS and DCS[7-9] may be explained by two factors: (i) the energy of P* is raised relative to E* in donor-donor-stilbenes (DDS) as compared to donor-stilbenes (DS) and donor-acceptor-stilbenes (DCS). Quantum chemical calculations to answer this point are underway; (ii) DDS may also populate a TICT (A*) state and thus energetically stabilize the original E* state by an excited state equilibrium. This view is supported by the fairly large excited-state dipole moment observed (Table II) although the compound is symmetric, and small dipole moments for both ground and excited state are expected. Further studies including bridged DDS model compounds may help to answer this question.

This study extends the results previously obtained for the DCS series.[7-9] All results can be explained within the same three-state model and provide additional evidence for the extensive importance of the single bond twist mechanism in polar arylethylene derivatives.

Acknowledgment. This work has been supported by BMFT project 05 414 FAB1 and the EC-Large Scale Installations Program (GE 1-0018-D(B)). We thank the donors of the Petroleum Research Fund, administered by the American Chemical Society, for financial assistance and T. Wolff, University of Siegen, for a sample of DS-B34.

Bond Dissociation Energies of 3,5,5- and 4,5,5-Trimethyl-2-oxomorpholines by Photoacoustic Calorimetry. An Assessment of the Additivity of Substituent Effects[1]

K. Brady Clark,[†] Danial D. M. Wayner,*[,†] Samuel H. Demirdji,[‡] and Tad H. Koch*[,‡]

Contribution from the Steacie Institute for Molecular Sciences, National Research Council of Canada, Ottawa, Ontario, Canada K1A 0R6, and Department of Chemistry and Biochemistry, University of Colorado, Boulder, Colorado 80309. *Received August 17, 1992*

Abstract: Carbon-hydrogen bond dissociation energies (BDE) and absolute rate constants for hydrogen atom abstraction by the *tert*-butoxyl radical have been measured for a number of aliphatic amines, including two captodatively substituted compounds (4,5,5-trimethyl-2-oxomorpholine (**1**) and 3,5,5-trimethyl-2-oxomorpholine (**2**)). The bond energies, determined by photoacoustic calorimetry, cover a range of about 15 kcal mol^{-1} (ca. 90 kcal mol^{-1} for the aliphatic amines to 75 kcal mol^{-1} for 4,5,5-trimethyl-2-oxomorpholine). The reactivity of the C-H bonds with the *tert*-butoxyl radical illustrates the importance of the stereoelectronic effect: in this case, conjugation between the incipient radical center and the developing π-system. In addition, there is evidence suggesting that relief of ring strain also plays an important role in determining both the BDE and the reactivity of the amine. The estimation of the captodative stabilization energies of the title compounds from BDE data is difficult for a number of reasons. The usual assumption that relative BDE(C-H) values are a measure of relative radical stabilization energies (RSE) is questioned. For cyclic esters evidence suggests that strain effects on the hydrocarbon versus those on the radical may have a significant effect. In addition, we have shown that the addition of RSE's from a methane based scale will overestimate the combined effect of two substituents on a C-H bond. We conclude that the method proposed originally by Benson provides a better estimate of multiple substituent effects on the BDE's. The analysis of the BDE's using this approach leads us to the conclusion that, for **1**, the substitutent effects on BDE(C-H) appear to be synergetic by ca. 9 kcal mol^{-1}. This should not be interpreted as a measure of the captodative effect on the radical since it is difficult to estimate the extent to which the relief of ring strain influences the BDE.

One of us has reported that the radicals 3,5,5-trimethyl-2-oxomorpholin-3-yl (TM-3) and 4,5,5-trimethyl-2-oxomorpholin-3-yl (TM-3′) exist in equilibrium with their respective dimers, at ambient temperatures, with steady state concentrations that are observable by EPR.[2-7] The C-C bond dissociation energies (BDE's) of the TM-3 and TM-3′ dimers in ethanol are 20.4 and

[†] National Research Council of Canada.
[‡] University of Colorado.

(1) Issued as NRCC publication No. 35241.
(2) Kleyer, D. L.; Haltiwanger, R. C.; Koch, T. H. *J. Org. Chem.* **1983**, *48*, 147-152.

0002-7863/93/1515-2447$04.00/0